 ©2014 Kvantovaya Elektronika and Turpion Ltd

PACS numbers: 42.72.Bj; 52.58.Lq
DOI: 10.1070/QE2014v044n11ABEH015611

EUV light source with high brightness at 13.5 nm

V.M. Borisov, K.N. Koshelev, A.V. Prokofiev, F.Yu. Khadzhiyskiy, O.B. Khristoforov

Abstract. **The results of the studies on the development of a high-brightness radiation source in the extreme ultraviolet (EUV) range are presented. The source is intended for using in projection EUV lithography, EUV mask inspection, for the EUV metrology, etc. Novel approaches to creating a light source on the basis of Z-pinch in xenon allowed the maximal brightness [130 W(mm^2 sr)$^{-1}$] to be achieved in the vicinity of plasma for this type of radiation sources within the 2% spectral band centred at the wavelength of 13.5 nm that corresponds to the maximal reflection of multilayer Mo/Si mirrors. In this spectral band the radiation power achieves 190 W in the solid angle of 2π at a pulse repetition rate of 1.9 kHz and an electric power of 20 kW, injected into the discharge.**

Keywords: *EUV source, radiation brightness, wavelength of 13.5 nm, EUV lithography, Z-pinch, xenon, discharge plasma.*

1. Introduction

The present-day projection lithography that allows one to create structures with element size smaller than tens of nanometres in large-scale production of integrated circuits (ICs) is one of the most widely used current nanotechnologies. The development of commercially approved projection lithography of new generation is based on using the sources of extreme ultraviolet radiation (EUV) at the wavelength of 13.5 nm that corresponds to the reflection maximum in multilayer Mo/Si mirrors [1, 2].

In the first EUV nanolithographs, operating in the test regime, the discharge radiation sources with the wavelength λ = 13.5 nm based on Z-pinch in xenon were used [3].

Although at present the use of discharge EUV radiation sources is not planned for large-scale production of new generation ICs, the problem of their development and improvement is still urgent. One of the promising applications of discharge EUV radiation sources is related to the inspection of lithography masks. The production of defectless masks and their diagnostics throughout the period of their exploitation play the most important role in the IC production technology, since, being present, the defects are projected onto the silicon substrate with the photoresist, making it unusable.

The masks for EUV lithography have a substrate with multilayer mirror coating that reflects at 13.5 nm, over which the topologic pattern made of material that absorbs at the same wavelength is deposited. In correspondence with the mask structure, several types of its defects can be distinguished that require different types of inspection, namely, the defects of the substrate (substrate inspection), the defects in the multilayer mirror coating (blank inspection), and the defects of the topologic pattern (pattern inspection). To detect and register the defects, one should perform the mask scanning, preferably with actinic radiation, the wavelength of which coincides with the operating wavelength of the nanolithograph. For this goal it is necessary to create a device based on an EUV source with high brightness $B_{13.5}$ = 30–100 W (mm^2 sr)$^{-1}$ in the spectral band near 13.5 nm (13.5 ± 0.135 nm), corresponding to the reflection band of multilayer mirrors, and the small value of the geometric factor (etendue) $E = S\Omega = 10^{-2}$–5×10^{-4}, where S is the area of the source in mm^2, and Ω is the solid angle of radiation output or collection in steradians. Every kind of inspection requires its own values of the parameters $B_{13.5}$ and E. The development of such a device and its key component, the high-brightness actinic source for inspecting the EUV masks, is among the priorities of the EUV lithography development.

A few companies and research teams in the world work at creating sources for diagnostics of lithography EUV masks and use different approaches to the solution of this problem.

In one of these approaches implemented in the source for inspecting EUV masks developed by the Federal Institute of Technology (Switzerland), the laser-induced plasma of Sn atoms generated under the action of the Nd:YAG laser radiation on the droplets of liquid tin is used [4]. The developers plan to increase the brightness $B_{13.5}$ of their source to nearly 200 W(mm^2 sr)$^{-1}$. One of the problems that should be solved to achieve this goal is how to provide the plasma spatial stability, hampered by the temporary jitter between the droplets and their lateral displacement. Another problem of the source based on the Sn plasma may be related to the great amount of polluting products present in it.

Alternative approaches to designing high-brightness sources of EUV radiation are based on using gas discharge Xe plasma. Thus, in the source developed by Energetiq Technology Inc. (USA) the induction or non-electrode Z-pinch in xenon is used. The maximal achieved brightness $B_{13.5}$ amounts to ~8 W (mm^2 sr)$^{-1}$, which is still lower than

V.M. Borisov, A.V. Prokofiev, O.B. Khristoforov 'EUV Labs' LTD, Sirenevyi blvd. 1, 142191 Troitsk, Moscow, Russia; Federal State Unitary Enterprise 'State Research Centre of Russian Federation – Troitsk Institute for Innovation and Fusion Research', ul. Pushkovykh 12, 142190 Troitsk, Moscow, Russia; e-mail khristofor@triniti.ru;
K.N. Koshelev 'EUV Labs' LTD, Sirenevyi blvd. 1, 142191 Troitsk, Moscow, Russia; Institute of Spectroscopy, Russian Academy of Sciences, ul. Fizicheskaya 5, 142190 Troitsk, Moscow, Russia; e-mail: kkoshelev4@gmail.com;
F.Yu. Khadjiyskiy 'EUV Labs' LTD, Sirenevyi blvd. 1, 142191 Troitsk, Moscow, Russia; e-mail: khadfedor@gmail.com

Received 6 July 2014
Kvantovaya Elektronika **44** (11) 1077–1082 (2014)
Translated by V.L. Derbov

required [5]. The pinch is produced in the SiC ceramic bush with the orifice diameter 3 mm, which makes it necessary to replace it periodically because of significant erosion [6].

In Ref. [7] the approach based on summation of radiation from several sources based on capillary discharge is proposed. The drawbacks of this approach can be associated with the source complexity and considerable erosion of the capillary ceramic wall that limits the operation lifetime.

One of the achievements in the field of source design for actinic inspection is the brightness $B_{13.5} = 12.9$ W(mm^2 sr)$^{-1}$ obtained in a compact high-brightness gas-discharge source developed by Fraunhofer Institute for Laser Technology (Germany) [8]. Its specific feature is the use of a hollow cathode discharge system that reduced the erosion, thus improving the reliability of the source and increasing its lifetime.

Besides the urgent applications for inspection of lithography masks, the relatively simple and compact high-brightness EUV sources based on X-pinch in xenon can be used for low-production EUV mini-scanners, as well as in EUV metrology.

The application fields of gas-discharge EUV sources, particularly, with Kr as a plasma-forming substance, include the microscopy and tomography of biologic objects in the spectral range of water transparency (from 2.4 to 4.4 nm) [9].

One more promising application is associated with the use of high-temperature pulsed plasma flows and high-energy photons, generated in the pinch-type discharge, for material surface processing [10].

In this paper we present the results of research and development of a high-power, high-brightness EUV radiation source based on modified Z-pinch in xenon with a ceramic-free discharge system, intended for the abovementioned applications. The work reported is one of the studies aimed at designing high-power discharge EUV radiation sources based on Xe and Sn plasma, performed by us in recent years [11–16], including those carried out in cooperation with Xtreme Technologies GmbH (Germany), Ushio Corp. (Japan), EPPRA SAS (France) and ASML (The Netherlands).

The present paper opens the series of publications devoted to the design and study of three types of high-brightness EUV sources based on the gas discharge plasma in the system with liquid metal electrodes and laser-induced plasma from liquid metal targets.

2. EUV source discharge system

Figure 1 presents a schematic diagram of the discharge system of the source, based on the modified X-pinch in xenon and having no ceramic insulator, commonly installed in the discharge region between a cathode (*1*) and an anode (*2*). In the discharge gap operating at a pressure of nearly 50 mTorr, which corresponds to the left branch of the Paschen curve for gases, the breakdown preferably occurs through the longer path, thus making it possible to use the slit gap (*4*) located at the periphery of the discharge region, as an insulator between the cathode and the anode. The slit gap (*4*) is connected with the evacuated vacuum chamber (*9*) via a set of holes (*5*), which in combination with the insulator (*6*) placed at a large distance from the discharge region provides reliable insulation between the cathode and the anode of the source.

Thus, the developed construction is free of the separating ceramic insulator, most critical in the sense of erosion, and only the metal of electrodes is subjected to erosion. To minimise the erosion, the copper cathode (*1*) and anode (*2*) are equipped with tungsten inserts (*7*) and are efficiently cooled

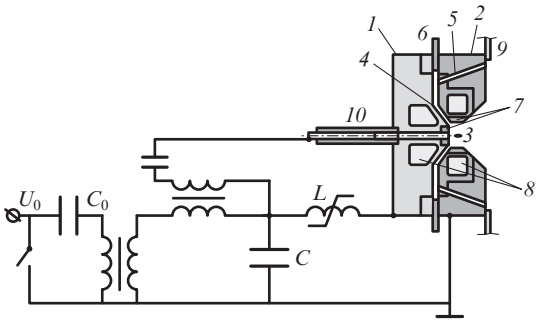

Figure 1. Schematic diagram of the EUV source based on Z-pinch with a ceramic-free electrode system.

with water flow (*8*). The spatial angle of the radiation output, determined by the configuration of the grounded electrode (*2*), amounts to 1.84 sr.

The working gas (xenon) is supplied through the central hole in the cathode. Preionisation is implemented on the inner surface of the ceramic tube (*10*) made of silicon nitride (Si_3N_4). The outlet of the gas from the electrode system and the radiation output occur into the vacuum chamber (*9*) equipped with two turbopumps.

3. Discharge plasma generation

To create high-current discharge Z-pinch with a high pulse repetition rate (up to 2 kHz) the power supply scheme with magnetic compression of the pump pulse was used. The scheme of a pulsed power supply provided the injection of energy into the discharge in the range of 7.5–21 J per pulse, the amplitude of the current pulse being from 36 to 59 kA.

In the pulsed power supply system (Fig. 1) the pulsed transformer is used that allows supporting optimal voltage on the load, different from the optimal operating voltage of the commutator, and implementing energy injection into the discharge using a single unipolar current pulse. Figure 2 presents typical oscillograms of the voltage U at the pulse-charged capacitor C, connected with the electrodes via the magnetic key L, and of the discharge current I.

For efficient emission in the spectral range near $\lambda = 13.5$ nm the plasma should possess the electron temperature 20–300 eV. The generation of high-temperature plasma in the scheme shown in Fig. 1 is implemented in the following way. When a high (~6 kV) voltage is applied to the preioniser, a creeping discharge is ignited on the inner surface of the ceramic tube (*10*). Between the plasma of the preioniser creeping discharge and the grounded electrode (*2*), and then between the high-voltage electrode (*1*) and the grounded electrode (*2*) the preliminary, relatively low-current (up to 5 kA) discharge is ignited, which is limited by the charge leakage current of the pulse-charged capacitor C through the magnetic key L, implemented as a low-inductance single-loop saturated choke. Due to the skin effect in the process of the pulsed prestrike having the duration of 1.5 μs the expanding axially symmetric current-plasma shell is formed that spreads into the off-axial part of the discharge region. The expansion of this shell stops at the slit gap (*4*) that hampers its further propagation and limits the discharge region, since the width of the slit gap is significantly smaller than the mean free path of electrons in the gas, so that the ionisation in the gap is absent. After the actuation of the magnetic key L (see Fig. 1)

the high-current stage of the pinch-type discharge is implemented, the duration of which amounts to 400 ns (Fig. 2). The current-plasma shell, created in the course of the prestrike, is compressed by a magnetic field of the pinch-type discharge current flowing on it, and during a short time appears to be confined to the axis of the discharge region. The plasma pinch, formed of the axis of the discharge region, emits short-wavelength radiation. The characteristic pulse duration for the radiation at the wavelength 13.5 nm amounted to 50 ns at the pulse half-maximum and 200 ns at the $1/e^2$ level.

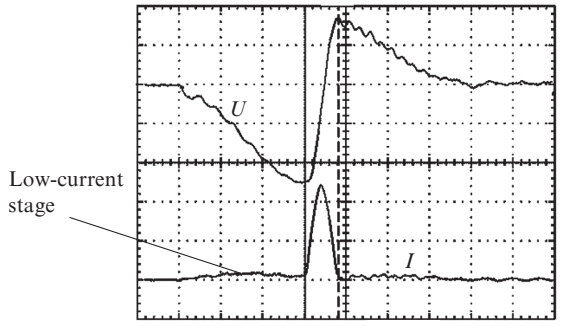

Figure 2. Oscillograms of the voltage U at the pulse-charged capacitor C and the discharge current I (inverted) with the amplitude values of –5 kV and –50 kA, respectively. The time scale is 500 ns div^{-1}.

The production of gas discharge plasma in the source of EUV radiation based on the modified Z-pinch using preionisation, a low-current forerunner pulse and excitation by a unipolar discharge current pulse improves the stability of EUV radiation from pulse to pulse, offers the possibility of making the volume of emitting plasma small, thereby providing high brightness and increasing the source efficiency.

4. Efficiency and power of the EUV source

The registration of the energy $E_{13.5}$ and the power $P_{13.5}$ of the EUV radiation in the spectral band 13.5 ± 0.135 nm was implemented using the meter with two Mo/Si mirrors and the AEUV-100 photodiode with a filter, blocking UV and visible radiation. The meter was calibrated using the etalon meter (Xtreme Technologies), calibrated at a synchrotron. Based on the measurements, the conversion efficiency $CE_{13.5}$ was calculated as a ratio of the energy, emitted in the spectral band 13.5 ± 0.135 nm into the solid angle 2π sr, and the electric energy E_{in}, injected into the discharge. The value of $CE_{13.5}$ depended mainly on the xenon pressure that was regulated using the gas leak valve (the standard leakage being 40–80 cm^3 min^{-1}).

According to the measurements of the EUV radiation intensity at the distance $l \approx 1.2$ m from the Z-pinch plasma at the optimal xenon pressure, $CE_{13.5} = 0.43\%$.

For $l \approx 0.82$ m the measured value of $CE_{13.5}$ increased to 0.54%. This is caused by a significant reduction of EUV radiation absorption in xenon in the case of putting the meter at a smaller distance from plasma. In this case, the measured pressure of Xe in the vacuum chamber amounted to ~0.88 Pa (6.6 mTorr).

One of the measurements at a distance $l \approx 0.82$ m from plasma was carried out with the meter paced in a 0.6 m long tube filled with flowing helium that absorbs EUV radiation insignificantly. The measured value of $CE_{13.5}$ in this case increased to 0.71%. The calculated estimate of the conversion efficiency directly near the plasma is $CE_{13.5} \approx 0.9\%$.

When the energy of EUV radiation was measured at two different distances from the plasma, we observed noticeable reduction of its absorption in the vacuum chamber with increasing pulse repetition rate (particularly, from 10 to 1800 Hz). The measured values of $CE_{13.5}$ for $f = 1800$ Hz were higher than for $f = 10$ Hz. This was explained by the formation of a hot gas plug in the discharge region at $f = 1800$ Hz that reduces the xenon output into the vacuum chamber, thereby reducing the absorption of the EUV radiation on its path ($l = 1.2$ m) to the meter.

These results show that due to significant absorption of radiation in xenon at the wavelength 13.6 nm in the vicinity of the plasma, the conversion efficiency $CE_{13.5}$ and the power of the EUV source radiation $P_{13.5}$ are two times higher than those, measured at a distance of 1.2 m from the source. As follows from the experiments, one of the efficient ways to increase $CE_{13.5}$ is to reduce the anode orifice through which xenon goes into the vacuum chamber. This is acceptable if the source is used for such applications as actinic inspection or metrology.

Below, unless specially indicated, the presented values of $CE_{13.5}$, $E_{13.5}$, and $P_{13.5}$ for the EUV source are obtained by direct measurements at the distance 1.2 m from the plasmas.

Figure 3 presents the dependence of $CE_{13.5}$ on E_{in} for the source operating regime with $f = 100$ Hz. It is seen that the maximal values of $CE_{13.5}$ are achieved in the wide range (from 9.5 to 16 J pulse^{-1}) of electric energy injected into the discharge, which was varied by changing the charging voltage of the power supply source. This means the possibility of efficient stabilisation of the EUV radiation power in the long-time operation regime by controlling the charging voltage.

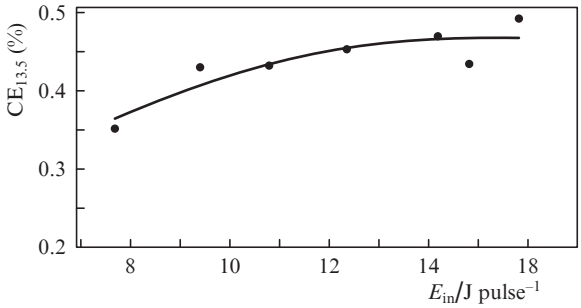

Figure 3. Conversion efficiency CE13.5 vs. energy E_{in} injected into the discharge at $f = 1000$ Hz.

Figure 4 presents the dependence of the EUV radiation power on the power $P_{in} = E_{in} f$ injected into the discharge in the continuous regime; each marked value of P_{in} corresponds to 5×10^6 pulses. For the maximal value of the injected power $P_{in} = 20.7$ kW at $f = 1.9$ kHz in the continuous regime, the maximal mean power of EUV radiation emitted into the solid angle 1.8 sr was found to be 34.7 W, i.e., $P_{13.5} = 34.7\,\mathrm{W}(1.8\ \mathrm{sr})^{-1}$. Being recalculated to the solid angle 2π, the source power amounts to 118.5 W$(2\pi\ \mathrm{sr})^{-1}$ in the case of direct measurement at the distance 1.2 m from the source. With the measured absorption of xenon taken into account, the EUV radiation power near the plasma amounts to 190 W$(2\pi\ \mathrm{sr})^{-1}$.

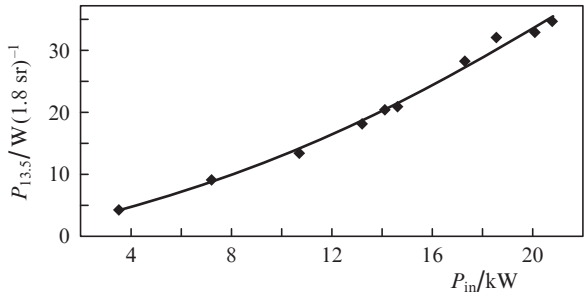

Figure 4. Power of the EUV radiation source vs. power injected into the discharge in the continuous regime.

5. The emitting plasma size and EUV source brightness

To optimise the EUV radiation source, its dimensions at different configurations of the electrode system and conditions of charge excitation were experimentally determined. Image recording and determination of dimensions for the plasma region that emits the EUV radiation were implemented by means of a pinhole camera with the 100 μm-wide aperture. The pinhole camera was equipped with a filter made of 200 nm thick Zn foil for eliminating the visible and UV radiation, the digital CCD array coated with a phosphorescent layer converting the EUV radiation into the detectable visible light, and the appropriate software. The registration scheme allowed both the imaging of a single pulse and obtaining an overlapped or averaged image of several pulses, forming a train with $f \leqslant 1000$ Hz. For simultaneous measurement of the longitudinal and transverse dimensions of the EUV radiation source the pinhole camera was installed at a sufficiently large (36.5°) angle with respect to the source axis.

As shown by the measurements, the dimensions of the image depend on the discharge geometry, xenon pressure and the electric energy injected into the discharge. Figure 5 presents the EUV source image recorded at the angle ~36.5° to the axis for the optimised geometry of electrodes (see Fig. 1) and an optimal xenon pressure, together with the profiles of its brightness B, obtained using a superposition of 10 sequential pulses with $f = 1000$ Hz and $E_{in} = 9.6$ J pulse^{-1}. In correspondence with the data of Fig. 5, the lateral dimension averaged over 10 pulses was estimated as 0.22 mm at the half-maximum and 0.53 mm at the $1/e^2$ level of brightness. The longitudinal dimensions were determined to be 1.4 and 2.8 mm, respectively. The dimensions of the radiation source are in good agreement with the requirements to the source aimed at EUV lithography.

The measurements with averaging over different numbers of pulses (from 2 to 20) have shown high spatial stability of the plasma region, emitting in the EUV range.

The measurements at different angles to the z axis gave the following values of the radiant intensity within the band

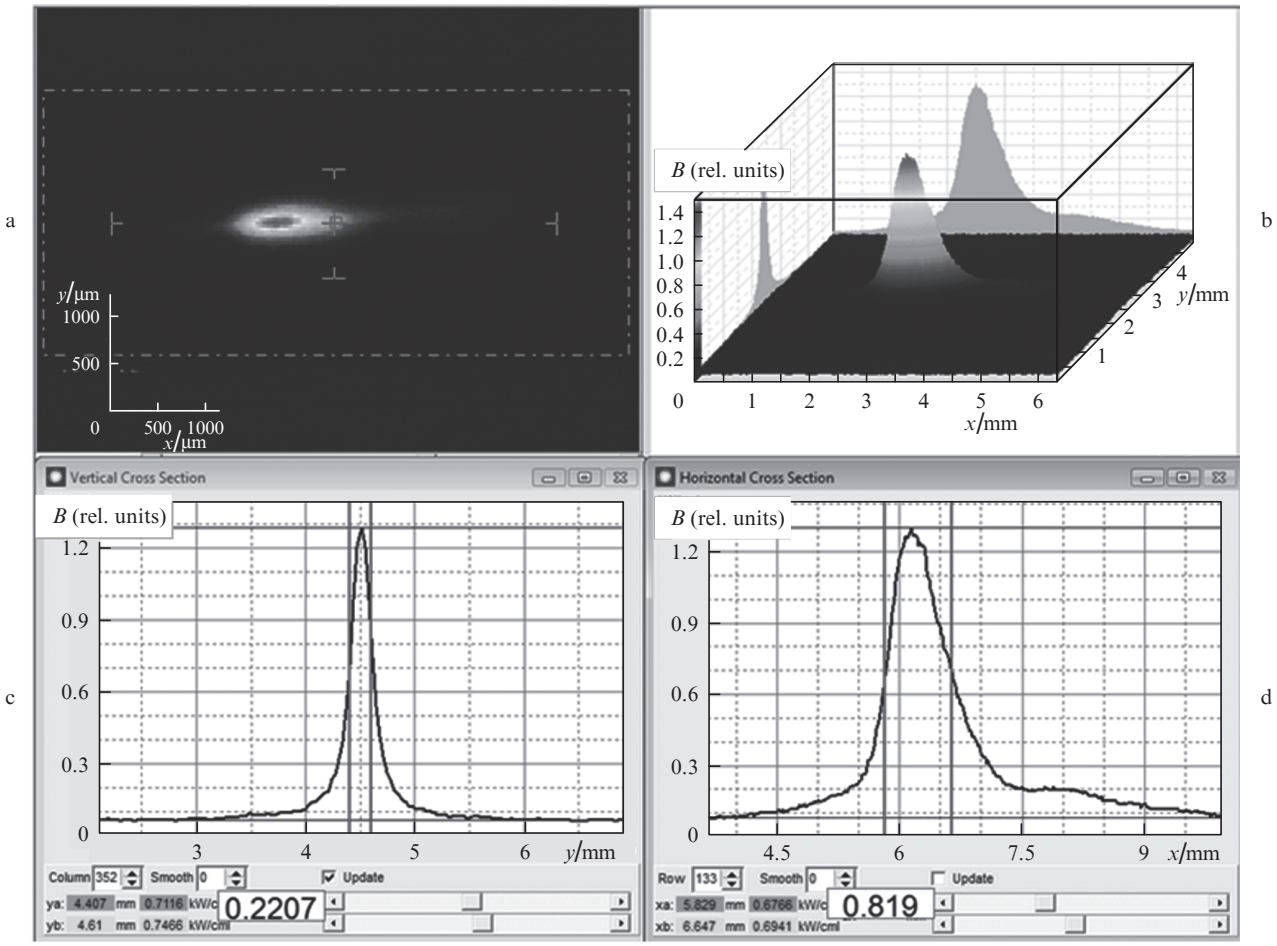

Figure 5. Image of the xenon plasma emitting in the EUV range, averaged over 10 pulses at $f = 100$ Hz, obtained at the angle 36.5° to the source axis (a), and the corresponding distributions of brightness – three-dimensional (b) and in two mutually perpendicular directions (c, d).

13.5 ± 0.135 nm at $l = 1.2$ m and $f = 1000$ Hz: 7.2 W sr^{-1} (40°), 7.2 W sr^{-1} (20°), 7.12 W sr^{-1} (7°) and 6.5 W sr^{-1} (0°). These results demonstrate the angular distribution of the EUV radiation intensity, close to an isotropic one.

The peak value of the brightness B_{peak} at the source axis was determined similar to [8] as

$$B_{peak} = \frac{CE_{13.5} f E_{in}}{\zeta \pi r_{1/2}^2},$$

where

$$\zeta = \frac{2\int_0^\infty f(r)\,dr}{r_{1/2}^2}$$

is the coefficient of normalised [$f(0) = 1$] profile of the source brightness, and $r_{1/2}$ is its radius at the half-maximum level.

For the values $r_{1/2} = 0.11$ mm, $\zeta = 3.9$, $CE_{13.5} = 0.39\%$ at $f = 100$ Hz and $E_{in} = 9.6$ J, measured at the axis of the source, the brightness of the EUV source was $B_{peak} = 40.2$ W (mm^2 sr)$^{-1}$. The power consumption for providing the brightness $B_{peak} \times (fE_{in})^{-1}$ in the spectral range 13.5 ± 0.135 nm amounts to 4.2 W (kW mm^2 sr)$^{-1}$.

In correspondence with these data, the estimated B_{peak} for the implemented operation regime with the injected power of 20 kW amounts to ~85 W (mm^2 sr)$^{-1}$ at the distance 1.2 m from the plasma, or about 135 W (mm^2 sr)$^{-1}$ in its immediate vicinity.

6. The source characteristics in the long-time operation regime

The studies have shown that the source with a ceramic-free electrode system (see Fig. 1) under the optimised conditions possesses not only high spatial stability, but also high energy stability. In a four-hour test of continuous operating regime with the mean injected power 9.6 kW and $f = 1000$ Hz, the relative instability σ of the EUV radiation pulse energy varied within the limits of 2.2%–1.5%.

Thanks to highly efficient water cooling, the source survived many hours of permanent operation with the injected electric power up to $P_{in} = 21$ kW without melting of electrodes.

However, the continuous operation time of the source was limited by erosion of electrodes, mainly the cathode that has a smaller, as compared to the anode, surface area in the vicinity of the central orifice, subject to extremely high thermal load. As a result, the cathode geometry changes due to erosion faster than that of the anode.

In the course of continuous operation of the EUV source with $f = 1.7$ kHz and $E_{in} = 8.2$ J pulse^{-1}, after 0.8×10^8 pulses the erosion of the cathode with the central orifice diameter 5 mm, determined by weighing before and after the test, amounted to 0.4×10^{-7} g pulse^{-1} (0.4×10^{-5} g C^{-1}). Replacing the cathode was enough to restore the source parameters. Figure 6 shows the behaviour of the source radiation power during the test with the injected power 10.5 kW at $f = 1100$ Hz. It is seen that the power is constant during the first 50×10^6 pulses, and then decreases by 13% during the next 40×10^6 pulses because of erosion. The pinch centre is gradually shifted towards the cathode by nearly 1 mm.

These studies have shown that in order to keep the output parameters of the EUV radiation source unchanged, it is necessary to replace at least the operating part of the cathode

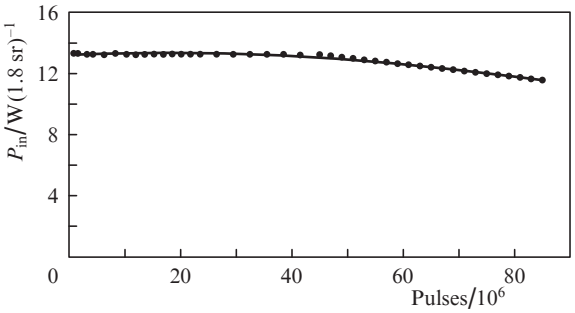

Figure 6. Dependence of the source radiation power on the number of pulses in the continuous regime at the injected power 10.5 kW and $f = 1100$ Hz.

approximately after each 50×10^6 pulses. The possibility of fast replacement of the electrode units and their restoration for further exploitation is provided by the developed construction of the source with the ceramic-free electrode system and the slit vacuum insulation between the electrodes.

7. Suppression of the corpuscular radiation flux

Since, alongside with the electromagnetic radiation, the discharge region generates a flux of pollutant particles (debris), a system of protection against the corpuscular radiation is to be installed between the radiation source and the optical collector. The system of protecting the optical collector, or debris mitigation tool (DMT), incorporates a combination of one or two traps, consisting of foil and buffer gas. Commonly the buffer gas, efficiently decelerating atoms and ions, is chosen to be argon or helium, as well as hydrogen under the pressure of a few Pa.

An advantage of the developed electrode system (see Fig. 1) is the absence of a ceramic insulator between the anode and the cathode, which can produce most debris. However, the peculiarities of the construction, related to using the slit insulation instead of separating ceramics, left open a question of the possibility to use efficiently the DMT with buffer gas.

The studies carried out in this connection have shown that the energy and spatial characteristics of the EUV source are not worsened by the installation of a water-cooled foil trap, similar to the one used in Ref. [3] with the argon protecting gas. The high mean power and brightness of the source were preserved after the introduction of an argon flow near the anode. It was shown that the vacuum insulation between the cathode and the anode is operable up to the argon pressure of 10 Pa, exceeding the pressure of protective gas, sufficient for efficient DMT use.

Besides, in the source operation an effect was found that depends on the gas pressure and affects the character of propagation of the debris particle flow from the zone of plasma formation. Under high pressures, optimal for the source operation, the observed effect was that more than 50% of the eroded electrode material returned to the anode and was collected on its butt non-working part. This effect, apparently, facilitates the protection of the collector optics against the pollution.

8. Conclusions

The performed studies aimed at the development of high-brightness source of EUV radiation based on Z-pinch in

xenon demonstrated the radiation power $P_{13.5}$ = 34.7 W (1.8 sr)$^{-1}$ at the distance l = 1.2 m from the plasma at P_{in} = 20.7 kW, f = 1.9 kHz in the continuous regime. According to the measured absorption of EUV radiation in xenon, the source power in the immediate vicinity of the plasma recalculated to the solid angle 2π approaches $\sim$190 W (2π sr)$^{-1}$. In correspondence with the known data [3], this is sufficient to support the EUV radiation power of 10–20 W in the intermediate focus.

The peak brightness of the EUV source, measured at the distance l = 1.2 m from the plasma, at P_{in} = 9.6 kW amounted to 40.2 W (mm^2 sr)$^{-1}$, and for the implemented operation regime with the injected power 20 kW it attained $\sim$8 W (mm^2 sr)$^{-1}$.

The obtained values of brightness are the highest known for gas-discharge sources of EUV radiation. This fact determines their promising applications in actinic (at λ = 13.5 nm) inspection of EUV masks, in EUV metrology, as well as in microscopy and tomography of biological objects.

Due to producing the modified Z-pinch with preionisation, low-current forerunner pulse, and excitation of discharge current with a unipolar pulse, the spatial and energy stability of the EUV source are improved. It is characterised by small (1.5 mm^2 sr) geometric factor, which meets the requirements to the source for EUV lithography, indicating the possibility to use it in a low-production EUV scanner.

The use of a ceramic-free discharge system reduces the flow of corpuscular debris from the region of plasma formation and, therefore, increases the reliability and lifetime of the source. We demonstrate the possibility of high-efficiency source operation in combination with a foil trap or DMT, as well as the development of new methods of suppressing corpuscular radiation of the discharge, based on the use of electromagnetic fields and controlled gas and plasma flows, which can supplement the existing methods.

To keep the output parameters of the EUV source stable, its construction should imply the possibility of rapid replacement of the electrode unit, which is necessary after each 50×10^6 pulses because of the electrode erosion. This is easily implementable in the developed construction with the slit insulation between the electrodes.

The obtained results agree with the data of Ref. [8] about the promising applications of high-brightness EUV sources based on Z-pinch in xenon for the actinic inspection.

At the same time we continue studying other approaches, free of drawbacks related to the limited lifetime of electrode systems in gas-discharge EUV sources. In further publications we plan to present the results of the work on constructing and studying high-brightness EUV sources based on, first, the plasma of laser-induces discharge between liquid metal electrodes and, second, the laser-induced plasma from liquid-metal targets.

Acknowledgements. The authors express their gratitude to Dr. Uwe Stamm, the ASML Vice President, for initiating the work, and to Vivek Bakshi, the EUV Litho Inc. President (USA), for his interest in this work.

The work was supported by the Ministry of Education and Science of the Russian Federation (Agreement No. 14.579.21.0004 of 05/06/2014 on the implementation of applied scientific research within the framework of the Federal Targeted Programme 'Research and Development in Priority Directions of Science and Technology Complex of Russia in 2014–2020', 'Development of Actinic Radiation Source for Inspecting Nanostructures in the Field of Nano- and Microelectronics' [unique identifier of applied research (project) RFMEFI57914X0004]. The work was also supported by the Russian Foundation for Basic Research (Grant No. 12-08-00528-a).

References

1. Banine V., Yakunin A., Glushkov D. *Proc. Intern. Workshop Extreme Ultraviolet Sources* (Dublin, Ireland, 13–15 November 2010).
2. Chkhalo N.I., Salashchenko N.N. *Proc. Intern. Workshop EUV and Soft X-Ray Sources* (Dublin, Ireland, 3–7 November 2013).
3. Stamm U., Kleinschmidt J., Bolshukhin D., Borisov V.M., et al. *Proc. SPIE Int. Soc. Opt. Eng.*, **6151**, 190 (2006).
4. Rollinger B., Gambino N., Giovannini A., Bozinova L., Alickaj F., Hertig K., Abhari R.S., Abreau1 F. *Proc. Intern. Workshop EUV and Soft X-Ray Sources* (Dublin, Ireland, 3–7 November 2013).
5. Gustafson D. *Proc. 2011 Intern. Workshop EUV Lithography* (Maui, Hawaii, 13–17 June 2011).
6. Gustafson D., Horne S.F., Besen M.M., Smith D.K., Partlow M.J., Blackborow P.A. *Proc. Intern. Workshop EUV and Soft X-Ray Sources* (Dublin, Ireland, 8–11 October 2012).
7. Zakharov S. *Proc. Intern. Workshop EUV and Soft X-Ray Sources* (Dublin, Ireland, 3–7 November 2013).
8. Benk M., Bergmann K. *J. Micro/Nanolith. MEMS MOEMS*, **11** (2), 021106 (2012).
9. Zahkarov V., Zahkarov S. *Proc. Intern. Workshop EUV and Soft X-Ray Sources* (Dublin, Ireland, 3–7 November 2013).
10. Borisov V.M., Kuzmenko V.A., Khristoforov O.B. *Inzh. Fiz.*, **4**, 34 (2014).
11. Borisov V., Eltsov A., Ivanov A., Khristoforov O., et al. *J. Phys. D Appl. Phys.*, **37**, 3254 (2004).
12. Borisov V.M., Vinokhodov A.Yu., Ivanov A.S., Kiryukhin Yu.B., Mishchenko V.A., Prokofiev F.V., Khristoforov O.B. *Kvantovaya Elektron.*, **39** (10), 967 (2009) [*Quantum Electron.*, **39** (10), 967 (2009)].
13. Borisov V., Eltsov A., Ivanov A., Khristoforof O., et al., in *Ref. EUV Sources for Lithography* (Washington: SPIE Press, 2006) p. 407.
14. Borisov V.M., Borisova G.N., Vinokhodov A.Yu., Zakharov S.V., Ivanov A.S., Kiryukhin Yu.B., Mishchenko V.A., Prokofiev A.V., Khristoforov O.B. *Kvantovaya Elektron.*, **40** (8), 720 (2010) [*Quantum Electron.*, **40** (8), 720 (2010)].
15. Banine V.Ye., Koshelev K.N., Swinkels G.H.P.M. *J. Phys. D Appl. Phys.*, **44**, 253001-1-18 (2011).
16. Banine V.Ye., Koshelev K.N., Swinkels G.H.P.M. *J. Micro/Nanolith. MEMS MOEMS*, **11** (2), 021112-1-6 (2012).